



OPEN

## Studies on solubility measurement of codeine phosphate (pain reliever drug) in supercritical carbon dioxide and modeling

Gholamhossein Sodeifian<sup>1,2,3</sup>✉, Chandrasekhar Garlapati<sup>4</sup>, Maryam Arbab Nooshabadi<sup>5</sup>, Fariba Razmimanesh<sup>1,2,3</sup> & Armin Roshanghias<sup>1,2,3</sup>

In this study, the solubilities of *codeine phosphate*, a widely used pain reliever, in supercritical carbon dioxide (SC-CO<sub>2</sub>) were measured under various pressures and temperature conditions. The lowest determined mole fraction of *codeine phosphate* in SC-CO<sub>2</sub> was  $1.297 \times 10^{-5}$  at 308 K and 12 MPa, while the highest was  $6.502 \times 10^{-5}$  at 338 K and 27 MPa. These measured solubilities were then modeled using the equation of state model, specifically the *Peng-Robinson model*. A selection of density models, including the *Chrastil model*, *Mendez-Santiago and Teja model*, *Bartle et al. model*, *Sodeifian et al. model*, and *Reddy-Garlapati model*, were also employed. Additionally, three forms of solid–liquid equilibrium models, commonly called expanded liquid models (*ELMs*), were used. The average solvation enthalpy associated with the solubility of *codeine phosphate* in SC-CO<sub>2</sub> was calculated to be  $-16.97$  kJ/mol. The three forms of the *ELMs* provided a satisfactory correlation to the solubility data, with the corresponding average absolute relative deviation percent (AARD%) under 12.63%. The most accurate *ELM model* recorded AARD% and AICc values of 8.89% and  $-589.79$ , respectively.

### List of symbols

$A_1, B_1$	Chrastil's model parameters (dimensionless, K)
$A_2, B_2, C_2$	MT model parameters (K, K m <sup>3</sup> /kg, dimensionless)
$A_3, B_3, C_3$	Bartle's model parameters (dimensionless, K m <sup>3</sup> /kg)
$A_4, B_4, C_4, D_4, E_4, F_5$	Sodeifian's model parameters (dimensionless, K/MPa <sup>2</sup> , m <sup>3</sup> /kg K, m <sup>6</sup> /kg <sup>2</sup> , 1/K MPa, K m <sup>3</sup> /kg)
$A_5, B_5, C_5, D_5, E_5, F_5$	Reddy-Garlapati's model parameters (all are dimensionless)
AARD%	Average absolute relative deviation percentage
AIC	Akaike information criterion
AIC <sub>c</sub>	Corrected AIC
$C_s$	The drug in the sample in vial (g/L)
D	Equation (27) parameter (J/molK)
E1 to E14	Symbols used in the experimental setup
$H_{sol}, H_{sub}, H_{total}$	Enthalpy (J/mol or kJ/mol)
$K_1, K_2, K_3$	Equation (10) parameters (m <sup>3</sup> /mol, m <sup>6</sup> /mol kg, m <sup>9</sup> /mol kg <sup>2</sup> )
$l_1, l_2, l_3$	Activity coefficient parameters (dimensionless, J/mole MPa, J <sup>2</sup> /mole <sup>2</sup> MPa <sup>2</sup> )
$M_{CO_2}, M_{Solute}$	The molar mass of CO <sub>2</sub> and drug solute (g/mol)
$n_{CO_2}$	CO <sub>2</sub> moles
$n_{drug}$	Drug moles
N	Data points
NIST	National Institute of Standards and Technology

<sup>1</sup>Department of Chemical Engineering, Faculty of Engineering, University of Kashan, Kashan 87317-53153, Iran. <sup>2</sup>Laboratory of Supercritical Fluids and Nanotechnology, University of Kashan, Kashan 87317-53153, Iran. <sup>3</sup>Modeling and Simulation Centre, Faculty of Engineering, University of Kashan, Kashan 87317-53153, Iran. <sup>4</sup>Department of Chemical Engineering, Puducherry Technological University, Puducherry 605014, India. <sup>5</sup>Bolvar Ghotbe Ravandi, Kashan Branch, Islamic Azad University, Ostaadan Street, Kashan 87159-98151, Iran. ✉email: sodeifian@kashanu.ac.ir

OF	Objective function
Q	Equation (32) parameter
P	Pressure (MPa)
$P_c, P_r$	Critical (Pa or MPa) and reduced pressures
$P_s$	Sublimation pressure (Pa or MPa)
R	Universal gas constant, 8.314 J/(mol K)
RMSD	Root mean square deviation
S	Solubility (kg/m <sup>3</sup> ; kg mol/m <sup>3</sup> )
SSE	The sum of squares error
SC-CO <sub>2</sub>	Supercritical carbon dioxide
T, T <sub>c</sub>	System temperature and critical temperature (K)
$v_1, v_2, v_3$	Molar volume (m <sup>3</sup> /mol)
$V_1, V_s$	Sampling loop and collection vial volumes, in (μL)
$y_2$	Drug solute solubility in mole fraction

### Greek symbols

$\beta$	Equation (11) parameters (dimensionless)
$\beta_1, \beta_2$ and $\beta_3$	Equation (30) parameters (J/K kg, J/K <sup>2</sup> kg and J/K <sup>3</sup> kg)
$\gamma$	Equation (11) parameters (K)
$\rho, \rho_r$	Density (kg/m <sup>3</sup> , kgmol/m <sup>3</sup> ), reduced density
$\kappa$	Association numbers
$\Delta_{sub}\delta$	Equation (11) parameters (dimensionless)

### Subscript

C	Critical
r	Reduced
Sol	Solvation
Sub	Sublimation
Total	Total

### Superscript

S	Saturation
---	------------

The importance of supercritical fluids (SCFs) as solvents in various processes has been recognized for decades<sup>1,2</sup>. Significant applications of SCFs encompass particle sizing, extraction, reactions, and separations<sup>3</sup>. SCFs serve as solvents in all of these applications<sup>3–6</sup>. However, it is essential to note that while theoretically, all substances can attain a supercritical state, some necessitate exceedingly high pressures and temperatures to achieve this state, rendering it impractical and resource-intensive<sup>7–10</sup>. Carbon dioxide is a well-known substance that readily reaches its supercritical state with minimal effort<sup>11–13</sup>. Consequently, CO<sub>2</sub> as an SCF is extensively documented in the literature<sup>14–16</sup>.

The sizing of drug particles, whether at the micro or nano level, primarily depends on their solubility<sup>17–20</sup>. The desired drug particle size can be achieved by rapidly expanding supercritical solutions (RESS) or anti-solvent processes<sup>21–23</sup>. The size of a drug particle can play a crucial role in treating various illnesses, as it significantly influences bioavailability<sup>24–28</sup>. Therefore, determining solubility is a fundamental step in micronization/nanonization. While recent literature reports the solubility of codeine phosphate in conventional solvents, information regarding its solubility in SCFs is notably absent<sup>29–31</sup>. Hence, this study focuses on measuring the solubility of codeine phosphate in supercritical carbon dioxide (SC-CO<sub>2</sub>) under various conditions. A modeling task is also undertaken to facilitate the application of the acquired data.

Several methodologies are available in the literature for modeling solubility data; however, only three are considered user-friendly<sup>32–34</sup>. The first method involves the use of the Equation of State (EoS), which requires critical properties of both the solute (the drug) and the solvent (SC-CO<sub>2</sub>). The second method relies on semi-empirical models, often referred to as density-based models, which necessitate data on the density of the solvent, as well as temperature and pressure data. The final method is the solid–liquid equilibrium model, also known as the expanded liquid model (ELM), which requires information about the solute's enthalpy of melting and the solute's melting temperature<sup>35–38</sup>. To obtain the required properties such as critical temperature, critical pressure, acentric factor, molar volume, and sublimation pressures, standard group contribution techniques are employed<sup>39–41</sup>. However, there are instances where the application of group contribution methods becomes challenging due to the absence of functional group contributions, such as phosphate and sulfates. Applying EoS modeling and the solid–liquid equilibrium model can prove challenging<sup>42–45</sup>. Codeine phosphate, an analgesic drug, exemplifies such a compound where critical properties ( $T_c$  and  $P_c$ ), molar volume ( $v_2$ ) and sublimation pressures are unavailable, and existing group contribution techniques cannot be applied due to the presence of phosphate in its structure. However, experimental data for the melting temperature (155 °C) and the heat of fusion (18.86 cal/g or 78.91 J/g or 31,358.83 J/mol) of codeine phosphate are readily accessible<sup>46–48</sup>. The magnitude of codeine phosphate's solubility in SC-CO<sub>2</sub> determines the technique employed for drug micronization/nanonization using SC-CO<sub>2</sub>.

The present work unfolds in two distinct phases. In the first phase, the solubilities of codeine phosphate in SC-CO<sub>2</sub> are measured under various conditions. The second phase evaluates the collected data using EoS, density, and ELM models.

## Experiment section

### Materials

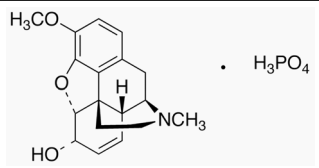
Codeine phosphate was provided by Parsian Pharmaceutical Co. (Tehran, Iran) with a CAS number of 52-28-8 and a mass purity exceeding 99%. CO<sub>2</sub> (carbon dioxide) with a CAS number of 124-38-9 and a mass purity exceeding 99.9% was supplied by Fadak Company, Kashan, Iran. Table 1 provides information about the chemicals used in this study.

### Equipment details

Static equipment was employed for solubility measurements, as depicted in Fig. 1. Comprehensive equipment details can be found in our previous studies<sup>49–51</sup>. This section offers a concise explanation of the experimental setup and methodology. Thermodynamically, the measurement method falls under the category of *isobaric-isothermal* methods<sup>52</sup>. Throughout the experiments, temperatures and pressures were rigorously controlled at the desired experimental conditions with a precision of  $\pm 0.1$  K for temperature and  $\pm 0.1$  MPa for pressure, respectively. Solubility measurements were conducted in triplicate for each data point. In each measurement, a known quantity of codeine phosphate drug (1 g) was utilized, and after reaching equilibrium, the saturated sample was collected through a 2-position 6-way port valve into a vial preloaded with demineralized water (DM water). After discharging 600  $\mu$ L of saturated SC-CO<sub>2</sub> the port valve was rinsed with 1 ml of DM water, resulting in a total saturation solution volume of 5 ml.

The drug solubility values were measured by absorbance assays at  $\lambda_{\max}$  (281 nm) on a UNICO-4802 UV-Vis spectrophotometer with 1-cm pass length quartz cells and the solubility was calculated from the concentration of solute by using the calibration curve (with regression coefficient 0.999) and the UV-absorbance, Fig. 2.

For solubility calculations, the following equations were employed:

Compound	Formula	Structure	M <sub>w</sub> (g/mol)	$\lambda_{\max}$ (nm)	CAS number	Minimum purity Mass fraction
Codeine phosphate	C <sub>18</sub> H <sub>21</sub> NO <sub>3</sub> · H <sub>3</sub> PO <sub>4</sub>		397.4	281	52-28-8	99%
Carbon dioxide	CO <sub>2</sub>		44.01		124-38-9	0.9999

**Table 1.** Molecular structure and physicochemical properties of used materials.

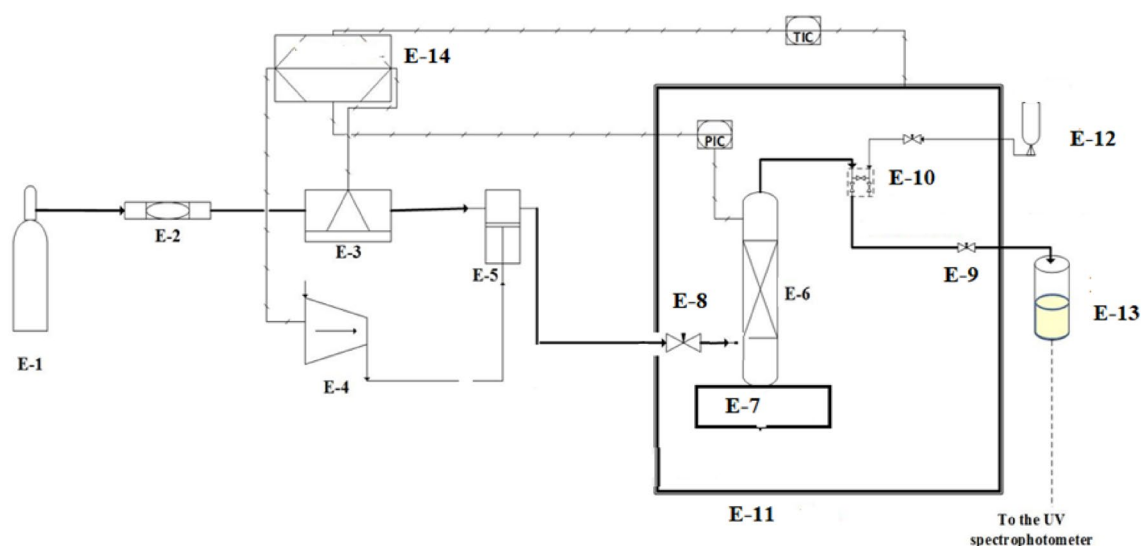


**Figure 1.** Experimental setup for solubility measurement, E1- CO<sub>2</sub> cylinder; E2- Filter; E3- Refrigerator unit; E4- Air compressor; E5- High pressure pump; E6- Equilibrium cell; E7- Magnetic stirrer; E8- Needle valve; E9- Back-pressure valve; E10- Six-port, two position valve; E11- Oven; E12- Syringe; E13- Collection vial; and E14- Control panel.

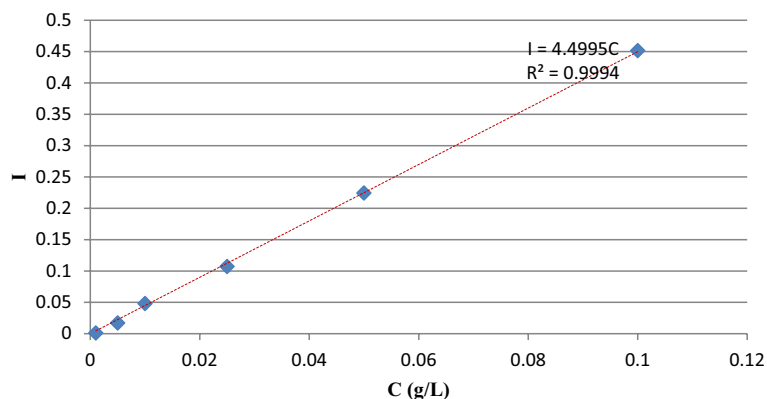


**Figure 2.** The calibration curve of drug in DM water.

$$y_2 = \frac{n_{drug}}{n_{drug} + n_{CO_2}} \quad (1)$$

where  $n_{drug}$  and  $n_{CO_2}$  represent the moles of codeine phosphate and  $CO_2$ , respectively. Moreover, these quantities are defined as follows:

$$n_{drug} = \frac{C_s \cdot V_s}{M_s} \quad (2)$$

$$n_{CO_2} = \frac{V_1 \cdot \rho}{M_{CO_2}} \quad (3)$$

In the above relations,  $C_s$  is defined as the drug concentration in saturated sample vial in g/L. Also, the volume of the sampling loop and vial collection are expressed as  $V_1(L) = 600 \times 10^{-6} \text{ m}^3$  and  $V_s(L) = 5 \times 10^{-3} \text{ m}^3$ , respectively. The  $M_s$  and  $M_{CO_2}$  are the molecular weights of the codeine phosphate drug (component 2) and  $CO_2$ , respectively.

Solubility can be also expressed as:

$$S = \frac{C_s V_s}{V_1} \quad (4)$$

where, one can find the relation between  $S$  and  $y_2$  as follows:

$$S = \frac{\rho M_s}{M_{CO_2}} \frac{y_2}{1 - y_2} \quad (5)$$

Codeine phosphate's solubility was determined using a UV-visible spectrophotometer (Model UNICO-4802, double beam, with multipurpose software, USA), with DM water as the solvent.

## Modeling

The solubility data obtained in this study were correlated with one equation of state (EoS), five density-based models, and three ELM models. we considered the Peng-Robinson (PR) EoS. In the case of density-based modeling, several well-known models, namely Chrastil, Mendez-Santiago, Teja (MT), Bartle et al., Sodeifian et al., and Reddy-Garlapati were employed. Three forms of ELMs with different parameters were used for data fitting. Detailed information about all the models considered in this work is discussed in the following sections.

### EoS modeling

This model is an extension to the model framework suggested by Schmitt<sup>53</sup> and Reid and Estévez et al.<sup>54</sup>. PR EoS was used for the modeling. Solubility of codeine phosphate (solute, component 2) in SC- $CO_2$  (solvent, component 1) is expressed as<sup>55</sup>

$$y_2 = \frac{P_2^s \hat{\phi}_2^s}{P \hat{\phi}_2^{SC-CO_2}} \exp \left[ \frac{(P - P_{2i}^s) v_s}{RT} \right] \quad (6)$$

where  $P_2^s$ ,  $\hat{\phi}_2^{SC-CO_2}$ ,  $\hat{\phi}_2^s P$ ,  $v_s$ ,  $T$  and  $R$ , are sublimation pressure, solid solute fugacity coefficient, saturation fugacity coefficient, system pressure, drug molar volume, system temperature and universal gas constant, respectively. The required equation for the solid solute fugacity coefficient in the SC- $CO_2$  ( $\hat{\phi}_2^{SC-CO_2}$ ) is calculated using PR EoS. It is obtained from the following thermodynamic equation.

$$\ln(\hat{\phi}_2^{SC-CO_2}) = \frac{1}{RT} \int_v^\infty \left[ \left( \frac{\partial P}{\partial N_i} \right)_{T,V,N_1} - \frac{RT}{v} \right] dv - \ln Z \quad (7)$$

Equation (8) represents the fugacity coefficients expression for PR EoS.

$$\ln(\hat{\phi}_2^{SC-CO_2}) = b_2/b(Z-1) - \ln(P(V-b)/RT) - a/(2\sqrt{2}RTb) \{ [2(a_{12}y_1 + a_2y_2)/a] - b_2/b \} \ln \left[ \frac{V + 2.414b}{V - 0.414b} \right] \quad (8)$$

For modeling tasks, critical temperature, critical pressure, centric factor, molar volume, and sublimation pressures of the codeine phosphate are required. Unfortunately, they are unavailable for this typical drug. Therefore, to overcome this drawback, the following assumptions are applied.

**Assumption 1** Solute in the solvent is very dilute. Thus, the required  $\hat{\phi}_2^{SC-CO_2}$  is obtained by applying William J. Schmitt and Robert C. Reid assumptions to Eq. (8) (i.e., for dilute system  $z \rightarrow z_1$ ,  $a \rightarrow a_1$  and  $b \rightarrow b_1$ ). Thus,  $\hat{\phi}_2^{SC-CO_2}$  PR EoS (Eq. 8) is reduced to Eq. (9). In which solute parameters are adjustable (i.e.,  $a_2$  and  $b_2$ )<sup>53</sup>.

$$\ln(\hat{\phi}_2^{SC-CO_2}) \approx b_2/b_1(Z_1-1) - \ln(P(V_1-b_1)/RT) - a_1/(2\sqrt{2}RTb_1) \{ [2(a_2)/a_1] - b_2/b_1 \} \ln \left[ \frac{V_1 + 2.414b_1}{V_1 - 0.414b_1} \right] \quad (9)$$

**Assumption 2** The molar volume of solute ( $v_2$ ) is a function of SC-CO<sub>2</sub> (solvent) density ( $\rho_1$ )<sup>56</sup> and in this work the following expression is used

$$v_2 = K_1 + K_2\rho_1 + K_3\rho_1^2 \quad (10)$$

where  $K_1, K_2, K_3$  have units are m<sup>3</sup>/mol, m<sup>6</sup>/mol kg, m<sup>9</sup>/mol kg<sup>2</sup>, respectively.

**Assumption 3** The sublimation pressure of the solute is expressed as a function of temperature, and it is expressed as Eq. (11)<sup>55</sup>

$$R \ln(P_A^{sub}) = \beta + \frac{\gamma}{T} + \Delta_{sub}\delta \ln\left(\frac{T}{298.15}\right) \quad (11)$$

where  $\beta, \gamma$  and  $\Delta_{sub}\delta$  are sublimation pressure expression coefficients. They are substituting Eqs. (9)–(11), in Eq. (6), results in the solubility model based on PR EoS in terms of pressure, temperature, density, and some adjustable parameters. The adjustable parameters are  $a_2, b_2, \beta, \gamma, \Delta_{sub}\delta, K_1, K_2$  and  $K_3$ . These parameters are treated as temperature-independent in the temperature range considered in the present work. The adjustable parameters are obtained by regression with experimental data.

For the data regression, the objective function, Eq. (12), is used<sup>57</sup>

$$OF = \sum_{i=1}^N \frac{|y_{2i}^{exp} - y_{2i}^{calc}|}{y_{2i}^{exp}} \quad (12)$$

where  $y_{2i}^{exp}$  is the experimental mole fraction of solute, and  $y_{2i}^{calc}$  is the model predicted mole fraction of solute.

### Density-based modeling

*Chrastil model*<sup>58–60</sup>

Solute concentration and solvent density are related as follows:

$$c_m = (\rho_{m1})^\kappa \exp\left(A_1 + B_1/T/K\right) \quad (13)$$

where  $c_m$  is the mass concentration of solute,  $\rho_{m1}$  is the mass concentration of solvent, and  $\kappa, A_1$  and  $B_1$  are model constants.

Equation (1) can be rearranged to mole fraction as follows:

$$\frac{c_m}{\rho_{m1}} \frac{M_{ScF}}{M_{Solute}} = \frac{M_{ScF}}{M_{Solute}} (\rho_1)^{\kappa-1} \exp\left(A_1 + B_1/T/K\right) \quad (14)$$

where  $M_{ScF}$ ,  $M_{Solute}$  and  $c_m/M_{Solute}$  are molar mass of SCF, molar mass of solute, and molar concentration of solute ( $c$ ), respectively. Also,  $\rho_{m1}/M_{ScF}$  and  $\kappa$  are molar concentration of solvent ( $\rho_1$ ), and association number, respectively. Furthermore,  $A_1$  and  $B_1$  are model constants.

$$\text{mole ratio} = \frac{c}{\rho_1} = \frac{M_{ScF}}{M_{Solute}} (\rho_1)^{\kappa-1} \exp\left(A_1 + B_1/T/K\right) \quad (15)$$

Mole fraction ( $y_2$ ) and mole ratios are related as follows:

$$\frac{c}{\rho_1} = \frac{y_2}{1 - y_2} \quad (16)$$

$$y_2 = \text{mole ratio} / [1 + \text{mole ratio}] \quad (17)$$

$$y_2 = \frac{M_{ScF}}{M_{Solute}} (\rho_1)^{\kappa-1} \exp\left(A_1 + B_1/T/K\right) / \left[1 + \frac{M_{ScF}}{M_{Solute}} (\rho_1)^{\kappa-1} \exp\left(A_1 + B_1/T/K\right)\right] \quad (18)$$

where  $\kappa, A_1$  and  $B_1$  are the model constants and their units are dimensionless, dimensionless and K, respectively.

#### Méndez-Santiago and Teja (MT) model<sup>61</sup>

This model can generally be used for checking thermodynamic consistency. It is stated as Eq. (19) and when  $T \ln(y_2 P) - C_2 T$  vs.  $\rho_1$  is established, all data points fall around a single straight line

$$T \ln(y_2 P) = A_2 + B_2 \cdot \rho_1 + C_2 T \quad (19)$$

where  $A_2, B_2$  and  $C_2$  are the model constants and their units are K, K m<sup>3</sup>/kg and dimensionless, respectively

#### Bartle et al. model<sup>62</sup>

According to the model, the solubility is expressed as Eq. (20)

$$\ln\left(\frac{y_2 \cdot P}{P_{ref}}\right) = A_3 + \frac{B_3}{T} + C_3(\rho_1 - \rho_{ref}) \quad (20)$$

where the pressure ( $P_{ref}$ ) and density for reference states ( $\rho_{ref}$ ) are considered 0.1 MPa, and 700 kg m<sup>-3</sup>. Also,  $A_3, B_3$  and  $C_3$  are the model constants and their units are dimensionless, K and m<sup>3</sup>/kg, respectively. From the constant  $B_3$ , sublimation enthalpy can be obtained (i.e.,  $\Delta_{sub}H = -B_3 R$  J/mol).

#### Sodeifian et al. model<sup>63</sup>

According to this model, the solubility is represented by Eq. (21)

$$y_2 = A_4 + B_4 \frac{P^2}{T} + C_4 \ln(\rho_1 T) + D_4 \rho_1 \ln(\rho_1) + E_4 P \ln(T) + F_4 \frac{\ln(\rho_1)}{T} \quad (21)$$

where  $A_4, B_4, C_4, D_4, E_4$  and  $F_4$  are the model constants and their units are dimensionless, K/MPa<sup>2</sup>, dimensionless, m<sup>3</sup>/Kg, 1/MPa and K, respectively.

#### Reddy-Garlapati model<sup>64</sup>

According to the model, the solubility is expressed as Eq. (22)

$$y_2 = (A_5 + B_5 P_r + C_5 P_r^2) T_r + (D_5 + E_5 P_r + F_5 P_r^2) \quad (22)$$

where  $A_5, B_5, C_5, D_5, E_5$  and  $F_5$  are the model constants and all are dimensionless quantities;  $P_r$  is reduced pressure and  $T_r$  is reduced temperature.

### Expanded Liquid Models (ELMs)

This section deals with models under the solid–liquid equilibrium model (also known as ELMs). It relies on the solution theory, where SC-CO<sub>2</sub> was considered an expanded liquid with infinite dissolved codeine phosphate. The essential solubility expression is given by<sup>65–68</sup>

$$y_2 = \frac{1}{\gamma_2^\infty} \frac{f_2^S}{f_2^L} \quad (23)$$

where  $\gamma_2^\infty$  is the activity coefficient of solute at infinite dilution,  $f_2^S, f_2^L$  are fugacity of codeine phosphate compound in the solid phase and expanded liquid phase, respectively. The basic equation for the fugacity ratio is represented by

$$\ln\left(\frac{f_2^S}{f_2^L}\right) = \frac{\Delta H_2^m}{RT} \left(\frac{T}{T_m} - 1\right) - \int_{T_m}^T \frac{1}{RT^2} \left[ \int_{T_m}^T [\Delta C_p] dT \right] dT \quad (24)$$

where  $\Delta C_p$  implies the difference between the heat capacity of solid and expanded liquid states. When Eqs. (23) and (24) are combined, the solubility expression for ELM is obtained as Eq. (25)

$$y_2 = \frac{1}{\gamma_2^\infty} \exp \left[ \frac{\Delta H_2^m}{RT} \left( \frac{T}{T_m} - 1 \right) - \int_{T_m}^T \frac{1}{RT^2} \left[ \int_{T_m}^T [\Delta C_p] dT \right] dT \right] \quad (25)$$

The solubility expression may be estimated with and without  $\Delta C_p$  term. In the following section, three cases are presented. For all three cases, a unique expression for  $\gamma_2^\infty$  used<sup>23,69</sup> was  $\exp(l_1 + l_2(p/(RT)) + l_3(p/(RT))^2)$ .

Case 1.  $\Delta C_p = 0$ .

The solubility expression for this case is written as

$$y_2 = \exp \left[ \frac{\Delta H_2^m}{RT} \left( \frac{T}{T_m} - 1 \right) \right] / \exp \left( l_1 + l_2 \left( \frac{p}{RT} \right) + l_3 \left( \frac{p}{RT} \right)^2 \right) \quad (26)$$

Thus Eq. (26) has three maximum parameters ( $l_1$ ,  $l_2$  and  $l_3$ ).

Case 2.  $\Delta C_p = \text{contant}$ . Consider the constant  $\Delta C_p$  is  $D$ <sup>23</sup>.

The solubility expression for this case is written as

$$y_2 = \exp \left[ \frac{\Delta H_2^m}{RT} \left( \frac{T}{T_m} - 1 \right) - D/R \left[ \ln \left( \frac{T}{T_m} \right) - T_m \left( \frac{1}{T_m} - \frac{1}{T} \right) \right] \right] / \exp \left( l_1 + l_2 \left( \frac{p}{RT} \right) + l_3 \left( \frac{p}{RT} \right)^2 \right) \quad (27)$$

Thus Eq. (27) has four maximum of parameters ( $D$ ,  $l_1$ ,  $l_2$  and  $l_3$ ) and respective units are J/mole K, dimensionless, J/mole MPa and J<sup>2</sup>/mole<sup>2</sup> MPa<sup>2</sup>, respectively.

Case 3.  $\Delta C_p = f(T)$ .

Generally,  $\Delta C_p$  it is a third-order polynomial equation in temperature equation; however, a recent study on solubility modeling shows that a good fit is achieved with the second-order polynomial. Thus, it is assumed that the  $\Delta C_p$  quadratic function in temperature as Eq. (28)<sup>70</sup>

$$\Delta C_p = \beta_1 + \beta_2 T + \beta_3 T^2 \quad (28)$$

Integral evaluation of Eq. (25) by substituting Eq. (28) results in Eq. (29)

$$\ln \left( \frac{f_2^S}{f_2^L} \right) = \frac{\Delta H_2^m}{RT} \left( \frac{T}{T_m} - 1 \right) - \frac{\beta_1}{R} \left[ \ln \left( \frac{T}{T_m} \right) - T_m \left( \frac{1}{T_m} - \frac{1}{T} \right) \right] - \frac{\beta_2}{2R} \left[ (T - T_m) - T_m^2 \left( \frac{1}{T_m} - \frac{1}{T} \right) \right] - \frac{\beta_3}{3R} \left[ \left( \frac{T^2}{2} - \frac{T_m^2}{2} \right) - T_m^3 \left( \frac{1}{T_m} - \frac{1}{T} \right) \right] \quad (29)$$

Thus, the solubility expression for this case is written as

$$y_2 = \exp \left[ \frac{\Delta H_2^m}{RT} \left( \frac{T}{T_m} - 1 \right) - \frac{\beta_1}{R} \left[ \ln \left( \frac{T}{T_m} \right) - T_m \left( \frac{1}{T_m} - \frac{1}{T} \right) \right] - \frac{\beta_2}{2R} \left[ (T - T_m) - T_m^2 \left( \frac{1}{T_m} - \frac{1}{T} \right) \right] - \frac{\beta_3}{3R} \left[ \left( \frac{T^2}{2} - \frac{T_m^2}{2} \right) - T_m^3 \left( \frac{1}{T_m} - \frac{1}{T} \right) \right] \right] / \exp \left( l_1 + l_2 \left( \frac{p}{RT} \right) + l_3 \left( \frac{p}{RT} \right)^2 \right) \quad (30)$$

In Eq. (30), six parameters are there and they are  $\beta_1, \beta_2, \beta_3, l_1, l_2$  and  $l_3$  and their units are J/K kg, J/K<sup>2</sup>kg, J/K<sup>3</sup>kg, dimensionless, J/mole MPa and J<sup>2</sup>/mole<sup>2</sup> MPa<sup>2</sup>, respectively. These parameters are optimally fitted to experimental solubility data by minimizing the error with the help of the objective function defined in Eq. (12). It is also important to note that all three expressions for solubility are explicit functions of composition.

## Results and discussion

The present study reports the measured solubilities of *codeine phosphate* ( $C_{18}H_{21}NO_3$ ) in supercritical carbon dioxide (SC-CO<sub>2</sub>) at temperatures of 308, 318, 328, and 338 K, spanning a pressure range of 12–27 MPa. Three types of models mentioned in the previous section were used in data correlation. The correlation task was carried out in *MATLAB 2019*<sup>®</sup> using the inbuilt *fminsearch* algorithm. The optimization algorithm minimized the error and was used for parameter estimation for all the models mentioned in the previous section. The measured data are shown in Table 2. The solvent density was obtained from the *NIST* database<sup>71</sup>. Considering the order of magnitude of *codeine phosphate* solubility in SC-CO<sub>2</sub>, supercritical anti-solvent methods can be regarded an appropriate choice for producing fine particles of this drug.

The solubility of *codeine phosphate* in SC-CO<sub>2</sub> vs. pressure is depicted in Fig. 3. From the solubility plot, it is evident that a cross-over pressure is not observed for *codeine phosphate*. Since conducting experimental investigations at each required condition (pressure and temperature) is tedious, modeling becomes necessary. Therefore, modeling was performed in all three modes. Numerous equations of state (EoS) are available in the literature for modeling solubility data. However, the PR EoS was selected in this work due to its success in modeling the solubilities of solid substances in supercritical fluids (SCFs)<sup>53–55,70</sup>. When correlating the data, the PR EoS model parameters were treated as temperature-independent over 308–338 K. The objective function indicated in Eq. (12) was utilized for data correlation, and all the adjustable parameters were obtained through regression with experimental data. Table 3 presents the correlation constants of the PR EoS model. Sublimation enthalpies at 308, 318, 328, and 338 K were calculated from the vapor pressure expression constants using the following relation:

Temperature (K) <sup>a</sup>	Pressure (MPa) <sup>a</sup>	Density of SC-CO <sub>2</sub> (kg/m <sup>3</sup> ) <sup>1</sup>	y <sub>2</sub> × 10 <sup>5</sup> (Mole fraction)	Experimental standard deviation, S( $\bar{y}$ ) × (10 <sup>5</sup> )	S (Equilibrium solubility) (g/L)	Expanded uncertainty of Mole fraction (10 <sup>5</sup> U)
308	12	769	1.297	0.021	0.090	0.072
	15	817	1.615	0.014	0.119	0.078
	18	849	1.702	0.022	0.131	0.086
	21	875	1.754	0.083	0.138	0.113
	24	896	1.897	0.031	0.153	0.104
	27	914	1.991	0.055	0.164	0.103
318	12	661	1.387	0.038	0.083	0.099
	15	744	2.614	0.091	0.176	0.041
	18	791	2.742	0.021	0.196	0.130
	21	824	3.158	0.077	0.235	0.108
	24	851	3.422	0.093	0.263	0.109
	27	872	3.817	0.040	0.300	0.106
328	12	509	1.891	0.082	0.087	0.115
	15	656	3.594	0.011	0.213	0.124
	18	725	3.949	0.088	0.259	0.150
	21	769	4.284	0.062	0.298	0.127
	24	802	4.521	0.095	0.327	0.176
	27	829	5.441	0.063	0.407	0.171
338	12	388	2.294	0.071	0.080	0.178
	15	557	3.959	0.081	0.199	0.142
	18	652	4.395	0.033	0.259	0.108
	21	710	4.927	0.128	0.316	0.137
	24	751	5.521	0.141	0.375	0.173
	27	783	6.502	0.065	0.459	0.115

**Table 2.** Solubility of crystalline codeine phosphatene SC-CO<sub>2</sub> at various temperatures and pressures. The experimental standard deviation was obtained by  $S(y_k) = \sqrt{\frac{\sum_{j=1}^n (y_j - \bar{y})^2}{n-1}}$ . Expanded uncertainty (U) and the relative combined standard uncertainty ( $u_{\text{combined}}/y$ ) are defined, respectively, as follows:  $(U) = k \cdot u_{\text{combined}}$  ( $k=2$ ) and  $u_{\text{combined}}/y = \sqrt{\sum_{i=1}^N (P_i u(x_i)/x_i)^2}$ . In this research,  $u(x_i)$  was considered as standard uncertainties of temperature, pressure, mole fraction, volumes and absorption.  $P_i$ , sensitivity coefficients, are equal to the partial derivatives of  $y$  equation (Eq. 1) with respect to the  $x_i$ . <sup>a</sup>Standard uncertainty  $u$  are  $u(T) = \pm 0.1$  K;  $u(p) = \pm 1$  bar. The value of the coverage factor  $k=2$  was chosen on the basis of the level of confidence of approximately 95 percent for calculating the expanded uncertainty.

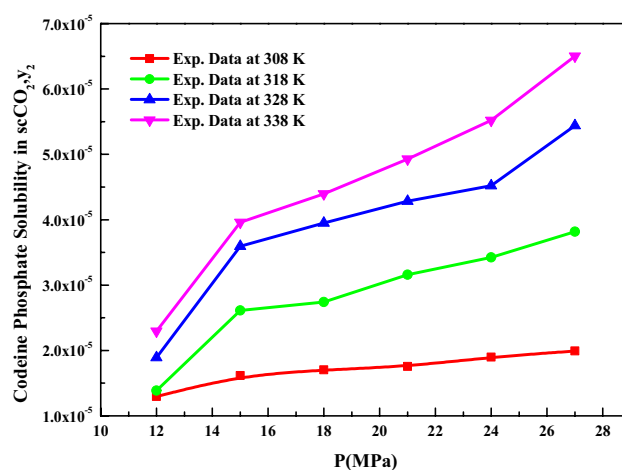


**Figure 3.** Codeine phosphate solubility in SC-CO<sub>2</sub>, y<sub>2</sub> versus P (MPa).



Name of the model	Parameters	AARD%	R <sup>2</sup>	R <sup>2</sup> <sub>adj</sub>
PREoS	$a_1 = 2.3463 \times 10^{-4}$	8.61	0.918	0.899
	$b_1 = 4.2013 \times 10^{-4}$			
	$\beta = 23.310$			
	$\gamma = -9127.5$			
	$\Delta_{sub}\delta = -5.9988$			
	$K_1 = 7.516 \times 10^{-4}$			
	$K_2 = -7.3793 \times 10^{-8}$			
$K_3 = -7.8339 \times 10^{-11}$				
Estimated Sublimation Enthalpies at T (K)	Sublimation Enthalpy (kJ/mol) Estimated using $\Delta_{sub}H = (-\gamma + \Delta_{sub}\delta T)R$	Average Sublimation Enthalpy in kJ/mol		
308	60.524	59.776		
318	60.026			
328	59.527			
338	59.028			

**Table 3.** Correlation constant of EoS model.

$$\Delta_{sub}H = (-\gamma + \Delta_{sub}\delta T)R \text{ J/mol} \quad (31)$$

The estimated sublimation enthalpies are presented in Table 3. The correlating ability of the *equation of state* (EoS) method is depicted in Fig. 3.

When considering density-based models for data correlation, the *Chrastil* model (Eq. 18), treated constants as independent variables, and their values were determined through regression with experimental data. The obtained constants are reported in Table 4. The correlating ability of the *Chrastil* model is illustrated in Fig. 4. Reasonable fit is observed when the data is represented as  $y_2$  versus  $\rho_1$ , this confirms the applicability of the *Chrastil* model to the solubility data<sup>72,73</sup>. From the parameters of the *Chrastil* model, the total enthalpy for *codeine phosphate* was derived, and its value is reported in Table 5.

The results for data fitting of the *MT model* (Eq. 19) are presented in Fig. 6, and the corresponding parameters are reported in Table 4. The correlating ability of the *MT model* is evident in Fig. 5, where linear plots are observed when the data is plotted as  $T/K \ln(y_2 \cdot P) - C_2T$  versus  $\rho_1$  (Fig. 6), this further confirms the suitability of the *MT model* for the solubility data<sup>72,73</sup>. Similarly, the model proposed by *Bartle et al.* (Eq. 20) was correlated with solubility data, and the obtained results are reported in Table 4. Linear plots are also observed when the data is

Name of the model	Parameters	AARD%	R <sup>2</sup>	R <sup>2</sup> <sub>adj</sub>
Chrastil	$\kappa = 2.8403$	9.48	0.902	0.897
	$A_1 = -4.0221$			
	$B_1 = -5284.7$			
MT model	$A_2 = -8817.9$	11.8	0.891	0.886
	$B_2 = 17.341$			
	$C_2 = 15.802$			
Bartle et al.	$A_3 = 17.257$	12.3	0.894	0.889
	$B_3 = -7326$			
	$C_3 = 5.2862 \times 10^{-3}$			
Sodeifan et al.	$A_4 = -0.015589$	8.52	0.936	0.933
	$B_4 = -3.2068 \times 10^{-5}$			
	$C_4 = 0.40046$			
	$D_4 = 1.1612 \times 10^{-3}$			
	$E_4 = -4.7474 \times 10^{-3}$			
$F_4 = -1005.1$				
Reddy and Garlapati	$A_5 = 1.68 \times 10^{-4}$	9.48	0.954	0.952
	$B_5 = -1.2939 \times 10^{-6}$			
	$C_5 = 2.2027 \times 10^{-5}$			
	$D_5 = -2.0904 \times 10^{-4}$			
	$E_5 = 3.8763 \times 10^{-5}$			
$F_5 = -2.8153 \times 10^{-5}$				

**Table 4.** Correlation constant of density-based models.

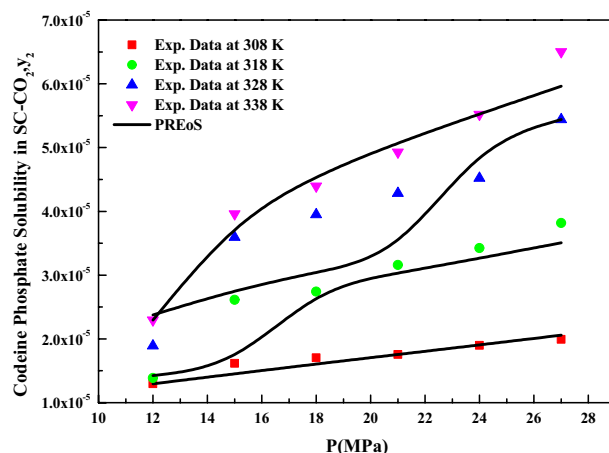


**Figure 4.** Codeine phosphate solubility in SC-CO<sub>2</sub>,  $y_2$  versus P (MPa). Symbols are experimental points; lines are PREoS model fit.

Model	Name of property		
	Total enthalpy $\Delta H_{\text{total}}$ (kJ/mol)	Enthalpy of sublimation $\Delta H_{\text{sub}}$ (kJ/mol)	Enthalpy of solvation $\Delta H_{\text{sol}}$ (kJ/mol)
Chrastil model	43.94 <sup>a</sup>		-16.97 <sup>d</sup>
Bartle et al. model		60.91 <sup>b</sup> (average value)	-15.84 <sup>e</sup>
PREoS		59.78 <sup>c</sup> (average value)	

**Table 5.** Thermodynamic parameters of codeine phosphate-SC-CO<sub>2</sub> system. <sup>d</sup>Obtained as a result of difference between  $\Delta H_{\text{sub}}$ <sup>b</sup> and  $\Delta H_{\text{total}}$ <sup>a</sup>. <sup>e</sup>Obtained as a result of difference between  $\Delta H_{\text{sub}}$ <sup>c</sup> and  $\Delta H_{\text{total}}$ <sup>a</sup>.

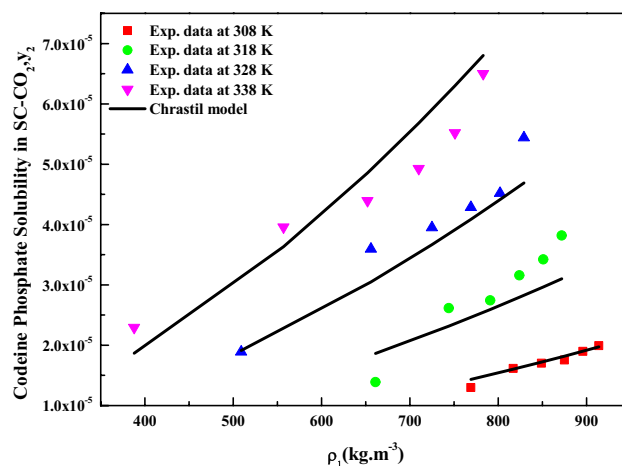


**Figure 5.** Codeine Phosphate Solubility,  $y_2$  versus  $\rho_1$ . Symbols are experimental points, and lines are Chrastil model fit.

represented as  $\ln(y_2 P / P_{\text{ref}})$  versus  $(\rho_1 - \rho_{\text{ref}})$  (Fig. 7), confirming the applicability of the *Bartle et al.* model to the solubility data<sup>72,73</sup>. From the parameters of the *Bartle et al.* model, the vaporization enthalpy was determined, and its value is reported in Table 5.

The solvation enthalpy was computed using the values of total and vaporization enthalpies, and the computed solvation enthalpy values are reported in Table 5. Notably, there is good agreement between the calculated average sublimation enthalpies from the *PR EoS* model (59.78 kJ/mol, as derived from Tables 3 and 5) and the calculated sublimation enthalpies from the *Bartle et al.* model (60.91 kJ/mol, as derived from Table 5). This suggests that using the *PR EoS* method in this study can yield meaningful correlation constants. However, the *PR EoS* accuracy decreases as the temperature increases from 308 to 338 K, possibly due to the temperature dependency of adjustable parameters. Figure 8 depicts the data fitting achieved using the *Sodeifian* and *Reddy-Garlapati* models.

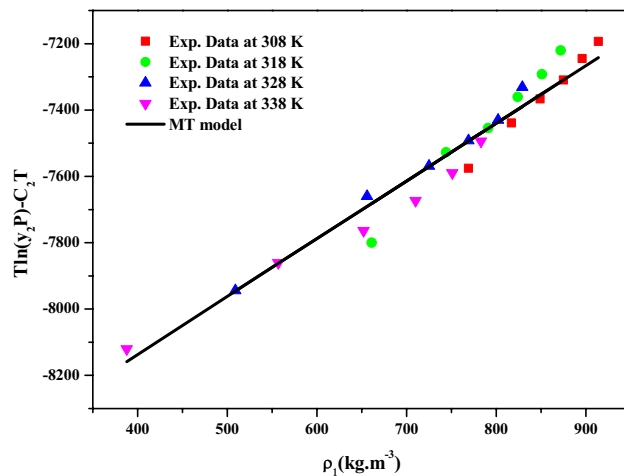


**Figure 6.**  $T \ln(y_2P) - C_2T$  vs.  $\rho_1(\text{kg m}^{-3})$ . Symbols are experimental points, and lines are MT model fit.

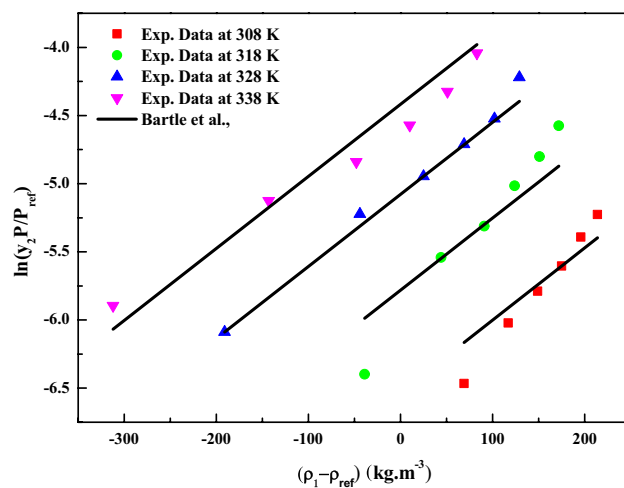


**Figure 7.**  $\ln(y_2P/P_{ref})$  versus  $(\rho_1 - \rho_{ref}) \text{kg m}^{-3}$ . Symbols are experimental points, and lines are Bartle et al., model fit.

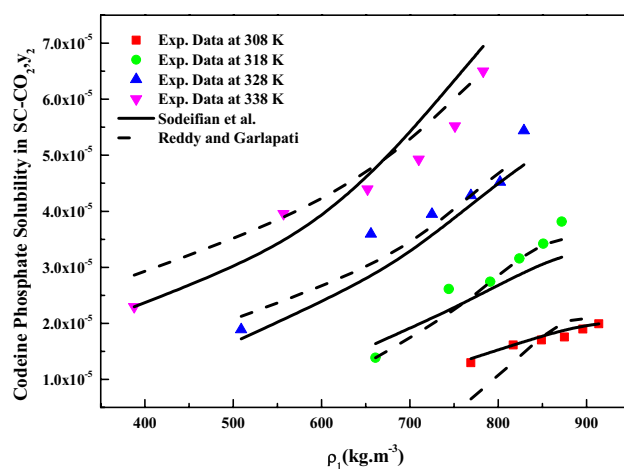


**Figure 8.** Codeine phosphate solubility in SC-CO<sub>2</sub>,  $y_2$  versus  $\rho_1(\text{kg m}^{-3})$ . Symbols are experimental points, lines are Sodefian and Reddy-Garlapati model's fit.

Three forms of expanded liquid models, precisely Eqs. (26), and (30), underwent evaluation with experimental data using the objective function mentioned in Eq. (12). Among these models, Eq. (30), which possesses the highest number of parameters, strongly agrees with the experimental data. Table 6 presents all the parameters associated with the expanded liquid models, and Fig. 9 shows the data correlation capabilities of these models.

The quality of data fit is contingent upon the number of parameters employed in the model. The Akaike Information Criterion (AIC) and the corrected AIC (AIC<sub>c</sub>) are utilized to discern the optimal model. AIC<sub>c</sub> is computed based on  $AIC^{74-77}$ , mathematical criteria commonly employed for assessing the compatibility of a solubility model with the corresponding solubility data. In statistics, these criteria compare solubility models and determine which best fits the data. AIC is appropriate when the data set comprises more than 40 data points, whereas AIC<sub>c</sub> is preferred when the data set contains fewer than 40 data points<sup>75,76</sup>. The following is relation between AIC and AIC<sub>c</sub>. Additionally, the adjustable or mode parameters may be determined by different algorithms or methods such as nonlinear regression models<sup>78,79</sup>.

$$AIC_c = AIC + \frac{2Q(Q+1)}{N-Q-1} \quad (32)$$

In Eq. (32),  $N$  represents the number of experimental data points,  $Q$  denotes the adjustable constants of the model, and  $AIC$  is defined as the sum of  $N \ln(SSE/N) + 2Q$ , where SSE stands for the sum of squared error. Table 7 displays all the computed values, revealing that Eq. (30) exhibits the lowest AIC<sub>c</sub> value, establishing it as the most suitable model for the given data.

The best model has the lowest AIC<sub>c</sub> value. The six-parameter ELM model is identified as the optimal choice, while based on AIC<sub>c</sub>, the Chrastil model exhibits a weaker correlation than the other models considered in this study.

Name of the model	Parameters	AARD%	R <sup>2</sup>	R <sup>2</sup> <sub>adj</sub>
ELM1	$l_1 = 10.134$	11.1	0.919	0.890
	$l_2 = -598.37$			
	$l_3 = 31,626$			
ELM2	$l_1 = 10.196$	11.0	0.919	0.891
	$l_2 = -600.81$			
	$l_3 = 31,962$			
	$D = -11.85$			
ELM3	$l_1 = 7.4325$	8.89	0.952	0.935
	$l_2 = -609.58$			
	$l_3 = 32,270$			
	$\beta_1 = 224,920$			
	$\beta_2 = -1269.3$			
	$\beta_3 = 13.166$			

**Table 6.** Correlation constant of ELM models.

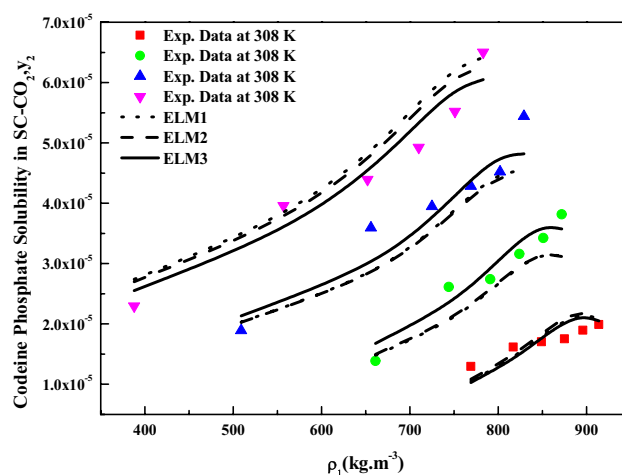


**Figure 9.** Codeine phosphate solubilities in SC-CO<sub>2</sub>,  $y_2$  versus  $\rho_1$  (kg m<sup>-3</sup>). Symbols are experimental points; lines are ELMs model's fit.

Name of the model	RMSE	SSE	AIC	AIC <sub>c</sub>
EoS model	$3.945 \times 10^{-6}$	$4.359 \times 10^{-10}$	-578	-567.97
Chrastil	$4.0383 \times 10^{-3}$	$3.5878 \times 10^{-4}$	-261	-259.46
MT model	$5.6176 \times 10^{-6}$	$6.9426 \times 10^{-10}$	-576	-575.19
Bartle et al.	$5.4034 \times 10^{-6}$	$6.4233 \times 10^{-10}$	-578	-577.06
Sodeifian et al.	$4.0748 \times 10^{-6}$	$3.6529 \times 10^{-10}$	-586	-580.86
Reddy-Garlapati	$3.3912 \times 10^{-6}$	$2.5301 \times 10^{-10}$	-595	-587.67
ELM1	$4.2894 \times 10^{-6}$	$4.4157 \times 10^{-10}$	-587	-586.05
ELM2	$4.2145 \times 10^{-6}$	$4.263 \times 10^{-10}$	-586	-583.99
ELM3	$3.2394 \times 10^{-6}$	$2.5185 \times 10^{-10}$	-595	-589.79

**Table 7.** Statistical values (AIC and AIC<sub>c</sub>) of all models.

## Conclusion

This research presents, for the first time, solubility data of *codeine phosphate* in *SC-CO<sub>2</sub>* measured at various conditions ranging between 308 and 338 K and 12–27 MPa. The measured data was found to vary within the range of  $(1.297–6.502) \times 10^{-5}$  in mole fraction. The obtained solubility data were modeled using the *PREoS* model, with solute properties as one of the adjustable constants. Among the density models, the *Chrastil*, *MT*, and *Bartle et al.* models effectively captured the data. From the model constants, the enthalpies of the *SC-CO<sub>2</sub>-codeine phosphate* mixture were determined. Three expanded liquid models (*ELMs*) were applied to the solubility data. The model results indicate that all the *expanded liquid models (ELMs)* reasonably fit the data compared to the *PR EOS* and density models. Finally, AIC<sub>c</sub> analysis indicates that the six-parameter *ELM model* is the most suitable model for data correlation. Considering the order of magnitude of solubility of *codeine phosphate* in *SC-CO<sub>2</sub>*, supercritical anti-solvent methods can be considered an appropriate choice for producing fine particles of this drug.

## Data availability

Upon request, the data can be obtained from the corresponding author.

Received: 8 June 2023; Accepted: 23 November 2023

Published online: 29 November 2023

## References

1. Taberero, A., del Valle, E. M. M. & Galán, M. A. Supercritical fluids for pharmaceutical particle engineering: Methods, basic fundamentals and modelling. *Chem. Eng. Process Intensif.* **60**, 9–25. <https://doi.org/10.1016/j.cep.2012.06.004> (2012).
2. Subramaniam, B., Rajewski, R. A. & Snavely, K. Pharmaceutical processing with supercritical carbon dioxide. *J. Pharm. Sci.* **86**(8), 885–890. <https://doi.org/10.1021/js9700661> (1997).
3. Mukhopadhyay, M. Partial molar volume reduction of solvent for solute crystallization using carbon dioxide as antisolvent. *J. Supercrit. Fluids* **25**(3), 213–223. [https://doi.org/10.1016/S0896-8446\(02\)00147-X](https://doi.org/10.1016/S0896-8446(02)00147-X) (2003).
4. Elvassore, N. K. Pharmaceutical processing with supercritical fluids. In *High Pressure Process Technology: Fundamentals and Applications* (ed. Bertucco, A.) 612–625 (Elsevier Science, 2001).
5. Gupta, R. B & Chattopadhyay, P. Method of forming nanoparticles and microparticles of controllable size using supercritical fluids and ultrasound. US patent No. 20020000681 (2002).
6. Reverchon, E., Adami, R., Caputo, G. & De Marco, I. Spherical microparticles production by supercritical antisolvent precipitation: interpretation of results. *J. Supercrit. Fluids* **47**(1), 70–84. <https://doi.org/10.1016/j.supflu.2008.06.002> (2008).
7. Sodeifian, G., Ardestani, N. S., Sajadian, S. A. & Panah, H. S. Experimental measurements and thermodynamic modeling of Coumarin-7 solid solubility in supercritical carbon dioxide: Production of nanoparticles via RESS method. *Fluid Phase Equilib.* **483**, 122–143. <https://doi.org/10.1016/j.fluid.2018.11.006> (2019).
8. Sodeifian, G., Sajadian, S. A., Ardestani, N. S. & Razmimanesh, F. Production of loratadine drug nanoparticles using ultrasonic-assisted rapid expansion of supercritical solution into aqueous solution (US-RESSAS). *J. Supercrit. Fluids* **147**, 241–253. <https://doi.org/10.1016/j.fluid.2018.05.018> (2019).
9. Sodeifian, G., Sajadian, S. A. & Ardestani, N. S. Determination of solubility of Aprepitant (an antiemetic drug for chemotherapy) in supercritical carbon dioxide: Empirical and thermodynamic models. *J. Supercrit. Fluids*. **128**, 102–111. <https://doi.org/10.1016/j.supflu.2017.05.019> (2017).
10. Sodeifian, G., Razmimanesh, F., Sajadian, S. A. & Hazaveie, S. M. Experimental data and thermodynamic modeling of solubility of Sorafenib tosylate, as an anti-cancer drug, in supercritical carbon dioxide: Evaluation of Wong-Sandler mixing rule. *J. Chem. Thermodyn.* **142**, 105998. <https://doi.org/10.1016/j.jct.2019.105998> (2020).
11. Sodeifian, G., Razmimanesh, F. & Sajadian, S. A. Prediction of solubility of sunitinib malate (an anti-cancer drug) in supercritical carbon dioxide (SC-CO<sub>2</sub>): Experimental correlations and thermodynamic modeling. *J. Mol. Liq.* **297**, 111740. <https://doi.org/10.1016/j.molliq.2019.111740> (2020).
12. Sodeifian, G. & Sajadian, S. A. Solubility measurement and preparation of nanoparticles of an anticancer drug (Letrozole) using rapid expansion of supercritical solutions with solid cosolvent (RESS-SC). *J. Supercrit. Fluids* **133**(1), 239–252. <https://doi.org/10.1016/j.supflu.2017.10.015> (2018).
13. Sodeifian, G., Razmimanesh, F., Ardestani, N. S. & Sajadian, S. A. Experimental data and thermodynamic modeling of solubility of Azathioprine, as an immunosuppressive and anti-cancer drug, in supercritical carbon dioxide. *J. Mol. Liq.* **299**, 112179. <https://doi.org/10.1016/j.molliq.2019.112179> (2019).
14. Hazaveie, S. M., Sodeifian, G. & Sajadian, S. A. Measurement and thermodynamic modeling of solubility of Tamsulosin drug (anti cancer and anti-prostatic tumor activity) in supercritical carbon dioxide. *J. Supercrit. Fluids* **163**, 104875. <https://doi.org/10.1016/j.supflu.2020.104875> (2020).

15. Sodeifian, G., Alwi, R. S., Razmimanesh, F. & Roshanghias, A. Solubility of pazopanib hydrochloride (PZH, anticancer drug) in supercritical CO<sub>2</sub>: Experimental and thermodynamic modeling. *J. Supercrit. Fluids* **190**, 105759. <https://doi.org/10.1016/j.supflu.2022.105759> (2022).
16. Sodeifian, G., Alwi, R. S., Razmimanesh, F. & Abadian, M. Solubility of Dasatinib monohydrate (anticancer drug) in supercritical CO<sub>2</sub>: Experimental and thermodynamic modeling. *J. Mol. Liq.* **346**, 117899. <https://doi.org/10.1016/j.molliq.2021.117899> (2022).
17. Sodeifian, G., Alwi, R. S., Razmimanesh, F. & Tamura, K. Solubility of quetiapine hemifumarate (antipsychotic drug) in supercritical carbon dioxide: Experimental, modeling and hansen solubility parameter application. *Fluid Phase Equilib.* **537**, 113003. <https://doi.org/10.1016/j.fluid.2021.113003> (2021).
18. Sodeifian, G., Garlapati, C., Razmimanesh, F. & Ghanaat-Ghamsari, M. Measurement and modeling of clemastine fumarate (antihistamine drug) solubility in supercritical carbon dioxide. *Sci. Rep.* **11**(1), 1–16. <https://doi.org/10.1038/s41598-021-03596-y> (2021).
19. Sodeifian, G., Nasri, L., Razmimanesh, F. & Abadian, M. CO<sub>2</sub> utilization for determining solubility of teriflunomide (immunomodulatory agent) in supercritical carbon dioxide: Experimental investigation and thermodynamic modeling. *J. CO<sub>2</sub> Util.* **58**, 101931. <https://doi.org/10.1016/j.jcou.2022.101931> (2022).
20. Sodeifian, G., Ardestani, N. S., Sajadian, S. A. & Panah, H. S. Measurement, correlation and thermodynamic modeling of the solubility of Ketotifen fumarate (KTF) in supercritical carbon dioxide: Evaluation of PCP-SAFT equation of state. *J. Fluid Phase Equilib.* **458**, 102–114. <https://doi.org/10.1016/j.fluid.2017.11.016> (2018).
21. Sodeifian, G., Detakhsheshpour, R. & Sajadian, S. A. Experimental study and thermodynamic modeling of Eesomeprazole (proton-pump inhibitor drug for stomach acid reduction) solubility in supercritical carbon dioxide. *J. Supercrit. Fluids* **154**, 104606. <https://doi.org/10.1016/j.supflu.2019.104606> (2019).
22. Sodeifian, G., Garlapati, C., Razmimanesh, F. & Sodeifian, F. Solubility of amlodipine besylate (calcium channel blocker drug) in supercritical carbon dioxide: Measurement and correlations. *J. Chem. Eng. Data* **66**(2), 1119–1131. <https://doi.org/10.1021/acs.jced.0c00913> (2021).
23. Sodeifian, G., Garlapati, C., Razmimanesh, F. & Sodeifian, F. The solubility of Sulfabenzamide (an antibacterial drug) in supercritical carbon dioxide: Evaluation of a new thermodynamic model. *J. Mol. Liq.* **335**, 116446. <https://doi.org/10.1016/j.molliq.2021.116446> (2021).
24. Sodeifian, G., Hazaveie, S. M., Sajadian, S. A. & Saadati Ardestani, N. Determination of the solubility of the repaglinide drug in supercritical carbon dioxide: Experimental data and thermodynamic modeling. *J. Chem. Eng. Data* **64**(12), 5338–5348. <https://doi.org/10.1021/acs.jced.9b00550> (2019).
25. Sodeifian, G., Hsieh, C.-M., Derakhsheshpour, R., Chen, Y.-M. & Razmimanesh, F. Measurement and modeling of metoclopramide hydrochloride (anti-emetic drug) solubility in supercritical carbon dioxide. *Arab. J. Chem.* <https://doi.org/10.1016/j.arabjc.2022.103876> (2022).
26. Sodeifian, G., Nasri, L., Razmimanesh, F. & Abadian, M. Measuring and modeling the solubility of an antihypertensive drug (losartan potassium, Cozaar) in supercritical carbon dioxide. *J. Mol. Liq.* **331**, 115745. <https://doi.org/10.1016/j.molliq.2021.115745> (2021).
27. Sodeifian, G., Razmimanesh, F., Sajadian, S. A. & Panah, H. S. Solubility measurement of an antihistamine drug (Loratadine) in supercritical carbon dioxide: Assessment of qCPA and PCP-SAFT equations of state. *Fluid Phase Equilib.* **472**, 147–159. <https://doi.org/10.1016/j.fluid.2018.05.018> (2018).
28. Sodeifian, G., Sajadian, S. A. & Razmimanesh, F. Solubility of an antiarrhythmic drug (amiodarone hydrochloride) in supercritical carbon dioxide: Experimental and modeling. *Fluid Phase Equilib.* **450**, 149–159. <https://doi.org/10.1016/j.fluid.2017.07.015> (2017).
29. Rezaei, H., Jouyban, A., Acree, W. E. Jr., Barzegar-Jalali, M. & Rahimpour, E. Solubility of codeine phosphate in cabitol +2-propanol mixtures at different temperatures. *Drug. Dev. Ind. Pharm.* **46**, 910–915. <https://doi.org/10.1080/03639045.2020.1762203> (2020).
30. Rezaei, H., Jouyban, A., Martinez, F., Barzegar-Jalali, M. & Rahimpour, E. Solubility of codeine phosphate in N-methyl-2-pyrrolidone+2-Propanol mixture at different temperatures. *J. Mol. Liq.* **316**, 113859. <https://doi.org/10.1016/j.molliq.2020.113859> (2020).
31. Rezaei, H., Kuentz, M., Zhao, H., Rahimpour, E. & Jouyban, A. Experimental, modeling and molecular dynamics simulation of codeine phosphate dissolution in N-methyl-2-pyrrolidone + ethanol. *Pharm. Sci.* <https://doi.org/10.34172/PS.2023.2> (2023).
32. Sodeifian, G., Garlapati, C., Hazaveie, S. M. & Sodeifian, F. Solubility of 2,4,7-triamino-6-phenylpteridine (triamterene, diuretic drug) in supercritical carbon dioxide: Experimental data and modeling. *J. Chem. Eng. Data* **65**(9), 4406–4416. <https://doi.org/10.1021/acs.jced.0c00268> (2020).
33. Sodeifian, G. *et al.* Solubility measurement and modeling of hydroxychloroquine sulfate (antimalarial medication) in supercritical carbon dioxide. *Sci. Rep.* **13**, 8112. <https://doi.org/10.1038/s41598-023-34900-7> (2023).
34. Sodeifian, G., Ardestani, N. S., Sajadian, S. A., Golmohammadi, M. R. & Fazlali, A. Solubility of sodium valproate in supercritical carbon dioxide: Experimental study and thermodynamic modeling. *J. Chem. Eng. Data* **65**(4), 1747–1760. <https://doi.org/10.1021/acs.jced.9b01069> (2020).
35. Sodeifian, G., Garlapati, C., Razmimanesh, F. & Nateghi, H. Experimental solubility and thermodynamic modeling of empagliflozin in supercritical carbon dioxide. *Sci. Rep.* **12**, 9008. <https://doi.org/10.1038/s41598-022-12769-2> (2022).
36. Sodeifian, G., Alwi, R. S. & Razmimanesh, F. Solubility of Pholcodine (antitussive drug) in supercritical carbon dioxide: Experimental data and thermodynamic modeling. *J. Fluid Phase Equilib.* **566**, 113396. <https://doi.org/10.1016/j.fluid.2022.113396> (2022).
37. Sodeifian, G., Sajadian, S. A. & Derakhsheshpour, R. Experimental measurement and thermodynamic modeling of Lansoprazole solubility in supercritical carbon dioxide: Application of SAFT-VR EoS. *Fluid Phase Equilib.* **507**, 112422. <https://doi.org/10.1016/j.fluid.2019.112422> (2020).
38. Sodeifian, G., Hazaveie, S. M., Sajadian, S. A. & Razmimanesh, F. Experimental investigation and modeling of the solubility of oxcabazepine (an anti convulsant agent) in supercritical carbon dioxide. *Fluid Phase Equilib.* **493**, 160–173. <https://doi.org/10.1016/j.fluid.2019.04.013> (2019).
39. Sodeifian, G. & Sajadian, S. A. Experimental measurement of solubilities of sertraline hydrochloride in supercritical carbon dioxide with/without menthol: Data correlation. *J. Supercrit. Fluids* **149**, 79–87. <https://doi.org/10.1016/j.supflu.2019.03.020> (2019).
40. Sodeifian, G., Usefi, M. M., Razmimanesh, F. & Roshanghias, A. Determination of the solubility of rivaroxaban (anticoagulant drug, for the treatment and prevention of blood clotting) in supercritical carbon dioxide: Experimental data correlations. *Arab. J. Chem.* **16**, 104421. <https://doi.org/10.1016/j.arabjc.2022.104421> (2023).
41. Abadian, M., Sodeifian, G., Razmimanesh, F. & Mahmoudabadi, S. Z. Experimental measurement and thermodynamic modeling of solubility of Riluzole drug (neuroprotective agent) in supercritical carbon dioxide. *Fluid Phase Equilib.* **567**, 113711. <https://doi.org/10.1016/j.fluid.2022.113711> (2023).
42. Sodeifian, G., Garlapati, C. & Roshanghias, A. Experimental solubility and modelling of crizotinib (anti cancer medication) in supercritical carbon dioxide. *Sci. Rep.* **12**, 17494. <https://doi.org/10.1038/s41598-022-22366-y> (2022).
43. Sodeifian, G., Alwi, R. S., Razmimanesh, F. & Sodeifian, F. Solubility of prazosin hydrochloride (alpha blocker antihypertensive drug) in supercritical CO<sub>2</sub>: Experimental and thermodynamic modeling. *J. Mol. Liq.* **362**, 119689. <https://doi.org/10.1016/j.molliq.2022.119689> (2022).
44. Sodeifian, G., Nasri, L., Razmimanesh, F. & Nooshabadi, M. A. Solubility of ibrutinib in supercritical carbon dioxide (Sc-CO<sub>2</sub>): Data correlation and thermodynamic analysis. *J. Chem. Thermodyn.* **182**, 107050. <https://doi.org/10.1016/j.jct.2023.107050> (2023).

45. Sodeifian, G., Hsieh, C.-M., Tabibzadeh, A., Wang, H.-C. & Nooshabadi, M. A. solubility of palbociclib in supercritical carbon dioxide from experimental measurement and Peng-Robinson equation of state. *Sci. Rep.* **13**, 2172. <https://doi.org/10.1038/s41598-023-29228-1> (2023).
46. Yang, L., Yin, H., Zhu, W. & Niu, S. Determination of codeine phosphate and codeine in thermal characterization by differential scanning calorimetry. *J. Therm. Anal.* **45**, 207–210. <https://doi.org/10.1007/BF02548681> (1995).
47. Roy, S. D. & Flynn, G. L. solubility and related physicochemical properties of narcotic analgesics. *Pharm. Res.* **5**, 580–586. <https://doi.org/10.1023/A:1015994030251> (1988).
48. Dahan, A. *et al.* Biowaiver monographs for immediate release solid oral dosage forms: Codeine phosphate. *J. Pharm. Sci.* **103**, 1592–1600. <https://doi.org/10.1002/jps.23977> (2014).
49. Sodeifian, G., Sajadian, S. A., Razmimanesh, F. & Hazaveie, S. M. Solubility of Ketoconazole (antifungal drug) in SC-CO<sub>2</sub> for binary and ternary systems: Measurements and empirical correlations. *Sci. Rep.* **11**(1), 1–13. <https://doi.org/10.1038/s41598-021-87243-6> (2021).
50. Sodeifian, G., Hazaveie, S. M. & Sodeifian, F. Determination of Galantamine solubility (an anti alzheimer drug) in supercritical carbon dioxide (CO<sub>2</sub>): Experimental correlation and thermodynamic modeling. *J. Mol. Liq.* **330**, 115695. <https://doi.org/10.1016/j.molliq.2021.115695> (2021).
51. Sodeifian, G., Ardestani, N. S., Razmimanesh, F. & Sajadian, S. A. Experimental and thermodynamic analysis of supercritical CO<sub>2</sub>- solubility of minoxidil as an antihypertensive drug. *Fluid Phase Equilib.* **522**, 112745. <https://doi.org/10.1016/j.fluid.2020.112745> (2020).
52. Peper, S., Fonseca, J. M. & Dohrn, R. High-pressure fluid-phase equilibria: Trends, recent developments, and systems investigated (2009–2012). *Fluid Phase Equilib.* **484**, 126–224. <https://doi.org/10.1016/j.fluid.2018.10.007> (2019).
53. Schmitt, W. J. & Reid, R. C. Solubility of monofunctional organic solids in chemically diverse supercritical fluids. *J. Chem. Eng. Data* **31**, 204–212. <https://doi.org/10.1021/je00044a021> (1986).
54. Estévez, L. A., Colpas, F. J. & Müller, E. A. A simple thermodynamic model for the solubility of thermolabile solids in supercritical fluids. *Chem. Eng. Sci.* **232**, 116268. <https://doi.org/10.1016/j.ces.2020.116268> (2021).
55. Garlapati, C. & Madras, G. Temperature independent mixing rules to correlate the solubilities of antibiotics and anti-inflammatory drugs in SCCO<sub>2</sub>. *Thermochim. Acta* **496**(1–2), 54–58. <https://doi.org/10.1016/j.tca.2009.06.022> (2009).
56. Iwai, Y., Koga, Y., Fukuda, T. & Arai, Y. Correlation of solubilities of high boiling components in supercritical carbon dioxide using a solution model. *J. Chem. Eng. Jpn.* **25**, 757–760. <https://doi.org/10.1252/jcej.25.757> (1992).
57. Valderrama, J. O. & Alvarez, V. H. Correct way of representing results when modelling supercritical phase equilibria using equation of state. *Can. J. Chem. Eng.* **83**(3), 578–581. <https://doi.org/10.1002/cjce.5450830323> (2008).
58. Chrastil, J. Solubility of solids and liquids in supercritical gases. *J. Phys. Chem.* **86**(15), 3016–3021. <https://doi.org/10.1021/j100212a041> (1982).
59. Sridar, R., Bhowal, A. & Garlapati, C. A new model for the solubility of dye compounds in supercritical carbon dioxide. *Thermochim. Acta* **561**, 91–97. <https://doi.org/10.1016/j.tca.2013.03.029> (2013).
60. Garlapati, C. & Madras, G. Solubilities of palmitic and stearic fatty acids in supercritical carbon dioxide. *J. Chem. Thermodyn.* **42**(2), 193–197. <https://doi.org/10.1016/j.jct.2009.08.001> (2010).
61. Méndez-Santiago, J. & Teja, A. S. The solubility of solids in supercritical fluids. *Fluid Phase Equilib.* **158**, 501–510. [https://doi.org/10.1016/S0378-3812\(99\)00154-5](https://doi.org/10.1016/S0378-3812(99)00154-5) (1999).
62. Bartle, K. D., Clifford, A., Jafar, S. & Shilstone, G. Solubilities of solids and liquids of low volatility in supercritical carbon dioxide. *J. Phys. Chem. Ref. Data* **20**(4), 713–756. <https://doi.org/10.1063/1.555893> (1991).
63. Sodeifian, G., Razmimanesh, F. & Sajadian, S. A. Solubility measurement of a chemotherapeutic agent (Imatinib mesylate) in supercritical carbon dioxide: Assessment of new empirical model. *J. Supercrit. Fluids* **146**, 89–99. <https://doi.org/10.1016/j.supflu.2019.01.006> (2019).
64. Reddy, T. A. & Garlapati, C. Dimensionless empirical model to correlate pharmaceutical compound solubility in supercritical carbon dioxide. *Chem. Eng. Technol.* **42**(12), 2621–2630. <https://doi.org/10.1002/ceat.201900283> (2019).
65. Kramer, A. & Thodos, G. Solubility of 1-hexadecanol and palmitic acid in supercritical carbon dioxide. *J. Chem. Eng. Data* **33**, 230–234. <https://doi.org/10.1021/je00053a002> (1988).
66. Iwai, Y., Koga, Y., Fukuda, T. & Arai, Y. Correlation of solubilities of high boiling components in supercritical carbon dioxide using a solution model. *J. Chem. Eng. Jpn.* **25**, 757–760. <https://doi.org/10.1252/jcej.25.757> (1992).
67. Alwi, R. S., Garlapati, C. & Tamura, K. Solubility of anthraquinone derivatives in supercritical carbon dioxide: new correlations. *Molecules* **26**(2), 460. <https://doi.org/10.3390/molecules26020460> (2021).
68. Kramer, A. & Thodos, G. Adaptation of the Flory-Huggins theory for modeling supercritical solubilities of solids. *Ind. Eng. Chem. Res.* **27**, 1506–1510. <https://doi.org/10.1021/ie00080a026> (1988).
69. Cabral, V. F., Santos, W. L. F., Muniz, E. C., Rubira, A. F. & Cardozo-Filho, I. Correlation of dye solubility in supercritical carbon dioxide. *J. Supercrit. Fluids* **40**, 163–169. <https://doi.org/10.1016/j.supflu.2006.05.004> (2007).
70. Mahesh, G. & Garlapati, C. Modelling of solubility of some parabens in supercritical carbon dioxide and new correlations. *Arab. J. Sci. Eng.* <https://doi.org/10.1007/s13369-021-05500-2> (2021).
71. National Institute of Standards and Technology. U.S. Department of Commerce, NIST ChemistryWebBook. <https://webbook.nist.gov/chemistry/>.
72. Garlapati, C. & Madras, G. Solubilities of some chlorophenols in supercritical CO<sub>2</sub> in the presence and absence of cosolvents. *J. Chem. Eng. Data* **55**(4), 273–277. <https://doi.org/10.1021/je900328c> (2010).
73. Ch. R., Garlapati, C. & Madras, G. Solubility of *n*-(4-Ethoxyphenyl) ethanamide in supercritical carbon dioxide. *J. Chem. Eng. Data* **55**(3), 1437–1440. <https://doi.org/10.1021/je900614f> (2010).
74. Akaike, H. Information theory and an extension of the maximum likelihood principle. In *Proceedings of the Second International Symposium on Information Theory* (ed Petrov, B.) 267–281 (Akademiai Kiado, Budapest, 1973).
75. Burnham, K. P. & Anderson, D. R. Multimodel inference: Understanding AIC and BIC in model selection. *Sociol. Methods Res.* **33**(2), 261–304. <https://doi.org/10.1177/0049124104268644> (2004).
76. Kletting, P. & Glatting, G. Model selection for time-activity curves: The corrected Akaike information criterion and the F-test. *Zeitschrift für medizinische Physik* **19**(3), 200–206. <https://doi.org/10.1016/j.zemedi.2009.05.003> (2009).
77. Anita, N. & Garlapati, C. A statistical analysis of solubility models employed in supercritical carbon dioxide. *AIP Conf. Proc.* **2446**, 180003. <https://doi.org/10.1063/5.0108200> (2022).
78. Hghtalab, A. & Sodeifian, G. Determination of the discrete relaxation spectrum for polybutadiene and polystyrene by a non-linear regression method. *Iran. Polym. J.* **11**, 107–113 (2002).
79. Sodeifian, G. & Haghtalab, A. Discrete relaxation spectrum and K-BKZ constitutive equation for PVC, NBR and their blends. *Appl. Rheol.* **14**, 180–189. <https://doi.org/10.1515/arh-2004-0010> (2004).

## Acknowledgements

We want to express our gratitude to the University of Kashan, Deputy of Research (Grant # Pajoothaneh-1402/5) for providing financial support.

### Author contributions

G.S. Conceptualization, Methodology, Validation, Investigation, Supervision, Project administration, Writing-review & editing; C.G. Methodology, Investigation, Software, Writing-original draft; M.A.N Validation, Measurement, Resources; F.R. Investigation, Software, Validation; A.R. Resources.

### Competing interests

The authors declare no competing interests.

### Additional information

**Correspondence** and requests for materials should be addressed to G.S.

**Reprints and permissions information** is available at [www.nature.com/reprints](http://www.nature.com/reprints).

**Publisher's note** Springer Nature remains neutral with regard to jurisdictional claims in published maps and institutional affiliations.



**Open Access** This article is licensed under a Creative Commons Attribution 4.0 International License, which permits use, sharing, adaptation, distribution and reproduction in any medium or format, as long as you give appropriate credit to the original author(s) and the source, provide a link to the Creative Commons licence, and indicate if changes were made. The images or other third party material in this article are included in the article's Creative Commons licence, unless indicated otherwise in a credit line to the material. If material is not included in the article's Creative Commons licence and your intended use is not permitted by statutory regulation or exceeds the permitted use, you will need to obtain permission directly from the copyright holder. To view a copy of this licence, visit <http://creativecommons.org/licenses/by/4.0/>.

© The Author(s) 2023